18th National and 7th ISHMT-ASME
Heat and Mass Transfer Conference
January 4-6, 2006
IIT Guwahati, India

Paper No. : SG02

A Fixed Grid Numerical Methodology for Modeling Wet Chemical Etching

P. Rath
School of Mechanical and Aerospace Engineering
Nanyang Technological University
Singapore-639798
Email: pe1756649@ntu.edu.sg

J. C. Chai[1]
School of Mechanical and Aerospace Engineering
Nanyang Technological University
Singapore-639798
Email: mckchai@ntu.edu.sg

H. Zheng
Singapore Institute of Manufacturing Technology
Singapore-638075
Email: hyzheng@SIMTech.a-star.edu.sg

Y. C. Lam
School of Mechanical and Aerospace Engineering
Nanyang Technological University
Singapore-639798
Email: MYClam@ntu.edu.sg

V. M. Murukeshan
School of Mechanical and Aerospace Engineering
Nanyang Technological University
Singapore-639798
Email: MMurukeshan@ntu.edu.sg

Abstract

A new mathematical model based on the total concentration approach is proposed for modeling wet chemical etching process. The proposed mathematical model is a fixed domain formulation of the etching problem. The governing equation based on the total concentration includes the interface condition too. The total concentration of etchant includes the reacted and the unreacted concentration of etchant. The unreacted etchant concentration is solved in both the etchant solution and the substrate (with zero unreacted etchant concentration). The reacted concentration of etchant is used to capture the etchfront during the progress of etching with time. Unlike the moving grid method, the etchfront is found implicitly with the total concentration method. Finite volume method is used to solve for the transient concentration distribution of etchant. The proposed method is applied from etching simple to complex geometries partially covered with mask. Results from the proposed approach are compared with the existing analytical and numerical solutions.

NOMENCLATURE

D	diffusion coefficient of etchant
M_{Sub}	molecular weight of the substrate
X, Y	non-dimensional coordinate directions
a	coefficient of the discretization equation
c	unreacted etchant concentration
c_R	reacted etchant concentration
$c_{R,\max}$	maximum possible value of the reacted concentration
c_T	total concentration
m	stoichiometric reaction parameter
t	time
t^*	non-dimensional time
$v_{\hat{n}}$	normal velocity of the etchant-substrate interface
x, y	coordinate directions

Greek Symbols

α	underrelaxation factor
β	non-dimensional etching parameter
∇	vector differential operator
Δt	time step
ρ_{Sub}	density of the substrate

Subscripts

Et	the etchant
Sub	the substrate
o	initial
P	control volume P
T	total

Superscripts

m	iteration number

[1] Author for correspondence

o previous time step

Introduction

Wet chemical etching (WCE) process involves the removal of material from the substrate surface by the application of a reactive liquid etchant to form a specific pattern on the substrate surface. This process has potential application in microelectronic industries in the fabrication of integrated circuit devices [1], MEMS devices [2] and sensors [3]. As etching progresses, the etched interface moves. Hence this process is regarded as a moving boundary problem. This process motivates to predict and understand the etching profile growth in designing a specific pattern on the substrate surface.

Various mathematical models have been proposed by different researchers to model the WCE process such as the analytical asymptotic solution [4, 5], the moving grid (MG) method [6, 8-10], the level-set method [11, 12], and the total concentration fixed grid (FG) method [14, 15]. Based on the rate of reaction, two possible cases of WCE process can exists namely- the diffusion-controlled (infinite reaction rate) and the reaction-controlled (finite reaction rate) etching. These two cases are studied in the modeling of one-dimensional [7, 9, 14, 15], two-dimensional [4-8, 10, 11, 13] and three-dimensional [12] WCE using the above analytical and numerical approaches.

The MG method is the widely used numerical method for modeling WCE process. In the MG method, the computational domain is limited to the space occupied by the etchant, which expands with time. Hence the computation mesh has to be regenerated at every time step. The mesh velocities have to be accounted for in the governing equation in terms of an extra convection term [6, 10]. Further an unstructured mesh system or a body-fitted grid system is needed to model multidimensional WCE.

Recently, Chai and co-workers [14, 15] presented a FG approach based on the total concentration of etchant to model WCE process. This method is analogous to the enthalpy method used in the modeling of melting/solidification processes [16, 17]. The total concentration is the sum of the unreacted etchant concentration and the reacted etchant concentration. The governing equation based on the total concentration includes the interface condition. The reacted etchant concentration is the measure of the etchfront position during the etching process. Unlike the MG method, the etchfront is found implicitly with the total concentration method. Since the grids are fixed, hence there is no grid velocity. Therefore, cartesian grid can be used to capture the complicated etchfront in multidimensional etching.

In this article, the total concentration FG method is applied to model one-dimensional (1-D), two-dimensional (2-D) and three-dimensional (3-D) diffusion-controlled WCE. The governing equation, the boundary conditions and the interface condition are described. A brief description on various ingredients of the proposed FG method is given. A brief description of the numerical method used to solve the governing equation is given. The overall solution procedure is then summarized. Discussions of the results obtained using the proposed FG method are presented. Some concluding remarks are given to conclude this article.

Problem Description and Governing Equation

A diffusion-controlled etching is studied in this article from simple to complex geometries. The diffusion-controlled etching is associated with infinitely fast reaction at the interface. Hence the etchant concentration at the etchant-substrate interface closes to zero. The schematic and computational domains for three test problems are shown in Figs. 1-3. In 2-D etching, a gap of width $2a$ is to be etched in a substrate as shown in Fig. 2a and in 3-D etching a cavity of square cross-section with dimension $2a \times 2a$ is to be etched in a substrate as shown in Fig. 3a. The origin of the coordinate system is set to the etchant-substrate interface at $t = 0$ for the 1-D problem and at the center of the gap for 2-D and 3-D problems. Since the problem is symmetrical about the origin in Figs. 2 and 3, only half of the domain is considered in 2-D etching (Fig. 2b) and one-quarter is considered in 3-D etching (Fig. 3b). The governing equation, the initial condition, the boundary conditions and the interface condition are presented next.

In the absence of convection, the etchant concentration within the etchant domain is governed by the mass diffusion equation given by

$$\frac{\partial c}{\partial t} = \frac{\partial}{\partial x_j}\left(D \frac{\partial c}{\partial x_j} \right) \qquad \text{in } \Omega(t),\ t > 0 \tag{1a}$$

where j varies from 1 to 3 for 1-D, 2-D and 3-D etching problems respectively and D is the diffusion-coefficient of etchant. The initial and boundary conditions are

$$c = c_o \qquad \text{in } \Omega(t),\ t = 0 \tag{1b}$$

$$c = c_o \qquad \text{on } \Gamma_1, \Gamma_2 \tag{1c}$$

$$\frac{\partial c}{\partial \hat{n}} = 0 \qquad \text{on } \Gamma_3 \text{ and } \Gamma_4 \tag{1d}$$

$$c = 0 \qquad \text{on } f(t) \text{ and } -\delta(t) \tag{1e}$$

where $\hat{n}$ in Eq. (1d) represents the normal to the surface. The interface condition, which gives the equation of motion of the interface, is given as

$$\vec{v} = -\frac{DM_{Sub}}{m\rho_{Sub}} \nabla c \tag{1f}$$

where $\vec{v}$ is the velocity of the etchant-substrate interface, M_{Sub} is the molecular weight of the substrate, ρ_{Sub} is the

density of the substrate and m is the stoichiometric reaction parameter of the etchant-substrate reaction.

The Total Concentration Method

The total concentration of etchant is defined as

$$c_T \equiv c + c_R \tag{2}$$

where c_T is the total concentration, c is the unreacted etchant concentration and c_R is the reacted etchant concentration respectively. Physically, c_R is the etchant concentration consumed in the reaction process. As such it is constant except at the etchant-substrate interface. This is used to capture the etchfront implicitly. The value of c_R changes from 0 to its maximum possible value of $c_{R,\max}$ in a control volume where etching is taking place. The maximum possible value of the reacted concentration termed $c_{R,\max}$, is the amount of etchant required per unit volume of substrate to dissolve the substrate during reaction. It is given as

$$c_{R,\max} = \frac{m\rho_{Sub}}{M_{Sub}} \tag{3}$$

The governing equation based on the total concentration is given by

$$\frac{\partial c_T}{\partial t} = \frac{\partial}{\partial x}\left(D\frac{\partial c}{\partial x}\right) + \frac{\partial}{\partial y}\left(D\frac{\partial c}{\partial y}\right) \tag{4}$$

Using Eq. (2), Eq. (4) can be written as

$$\frac{\partial c}{\partial t} = \frac{\partial}{\partial x}\left(D\frac{\partial c}{\partial x}\right) + \frac{\partial}{\partial y}\left(D\frac{\partial c}{\partial y}\right) - \frac{\partial c_R}{\partial t} \tag{5}$$

The above equation is valid in both the etchant and the substrate regions. The interface condition given by Eq. (1f) is contained in Eq. (5) implicitly. A procedure to update the reacted concentration (c_R) is needed to complete the formulation. This is discussed next.

Procedure to Update c_R

In the proposed FG method, the etching-control-volumes (ECV) are first identified. The ECVs are the substrate control volumes adjacent to the etchant control volumes where the reaction between the etchant and the substrate is taking place. In an ECV, c_R changes from 0 to its maximum possible value of $c_{R,\max}$. The finite volume discretization equation (using the fully implicit scheme) of Eq. (5) for an ECV (control volume P) is given as

$$a_P c_P^m = \sum a_{nb} c_{nb}^m + a_P^o c_P^o - (c_{R,P}^m - c_{R,P}^o)\frac{\Delta V_P}{\Delta t} \tag{6}$$

where m is the m^{th} iteration of the current time step, o is the previous time step, P is the control volume P, nb is the neighboring control volumes, a is the coefficients of the discretization equation, ΔV is the volume of a control volume and Δt is the time step respectively. It is to be noted that Eq (6) is valid for all control volumes. Since, c_R is constant in the etchant and substrate regions, the last term on the right side of Eq. (6) is zero except in the ECV. At the $(m+1)^{\text{th}}$ iteration, Eq. (6) can be written as

$$a_P c_P^{m+1} = \sum a_{nb} c_{nb}^{m+1} + a_P^o c_P^o - (c_{R,P}^{m+1} - c_{R,P}^o)\frac{\Delta V_P}{\Delta t} \tag{7}$$

Subtracting Eq. (7) from Eq. (6) and rearranging, gives

$$c_{R,P}^{m+1} = c_{R,P}^m + \frac{\Delta t}{\Delta V_P}\left[a_P(c_P^m - c_P^{m+1}) + \sum a_{nb}(c_{nb}^{m+1} - c_{nb}^m)\right] \tag{8}$$

When the solution converges, the last term of Eq. (8) will be zero. However, during the initial iteration process, it is most likely a non-zero term. Realizing that it is zero upon convergence, this term can be ignored from the calculation and Eq. (8) becomes

$$c_{R,P}^{m+1} = c_{R,P}^m + \alpha\, a_P \frac{\Delta t}{\Delta V_P}(c_P^m - c_P^{m+1}) \tag{9}$$

where α is an under-relaxation factor. For a diffusion-controlled reaction, the reaction rate at the interface is infinitely fast which makes the concentration at the interface zero. For diffusion-controlled reaction, the proposed FG procedure ensures that $c_P^{m+1} = 0$ and the excess concentration is used to update the reacted concentration. With $c_P^{m+1} = 0$, Eq. (9) becomes

$$c_{R,P}^{m+1} = c_{R,P}^m + \alpha\, a_P \frac{\Delta t}{\Delta V_P} c_P^m \tag{10}$$

In the ECVs, the reacted concentration is updated using Eq. (10). Etching for a given ECV completed, when $c_{R,P}^{m+1}$ reaches $c_{R,\max}$.

Numerical Method

In this article, the finite-volume method (FVM) of Patankar [18] is used to solve the diffusion equation (Eq. 5). Since a detailed discussion of the FVM is available in Patankar [18], only a brief description of the major features of the FVM used is given here. In the FVM, the domain is divided into a number of control volumes such that there is one control volume surrounding each grid point. The grid point is located in the center of a control volume. The governing equation is integrated over each control volume to derive an algebraic equation containing the grid point values of the dependent variable. The discretization equation then expresses the conservation principle for a finite control volume just as the partial differential equation expresses it for an infinitesimal control volume. The resulting solution implies that the integral conservation of mass is exactly satisfied for any control volume and of course, for the whole domain. The resulting algebraic equations are solved using a line-by-line Tri-Diagonal Matrix Algorithm. In the present study, a solution is deemed

converged when the maximum change in the concentration and the maximum change in the reacted concentration between two successive iterations are less than 10^{-11}.

Overall Solution Procedure

The overall solution procedure for the proposed total concentration method can be summarized as follows:

1. Specify the etchant domain, the substrate domain and the mask region. Ensure that the etchant-substrate interface lies on the interface between two control volumes.
2. Set the initial etchant concentration as c_o in the etchant domain and zero in the substrate domain including the mask region.
3. Initially set c_R to 0 in the substrate domain including the mask region and to $c_{R,max}$ in the etchant domain respectively.
4. Advance the time step to $t + \Delta t$.
5. Identify the etching control volumes (ECVs).
6. Use the "internal" boundary condition treatment of Patankar [18] (by setting S_P to a big number) to set the unreacted etchant concentration in the mask and substrate regions to zero.
7. Set S_P in the ECV to zero.
8. Solve Eq. (5) for the unreacted concentration.
9. Update the reacted concentration in the ECVs using Eq. (10).
10. Check for convergence.
    a) If the solution has converged, then check if the required number of time steps has been reached. If yes, stop. If not repeat (4) to (10).
    b) If the solution has not converged, then check the calculated reacted concentration.
        - If $c_R < c_{R,\max}$, repeat (8) to (10).
        - If $c_R \geq c_{R,\max}$, then set $c_R = c_{R,\max}$ and repeat (5) to (10).

Results and Discussions

Three test problems namely 1-D, 2-D, and 3-D etching are illustrated using the proposed FG method for modeling diffusion-controlled etching. The schematic of the test problems and the computational domains are shown in Figs. 1-3. In 2-D etching, a gap of width $2a$ and in 3-D etching, a gap of square cross-section with dimension $2a \times 2a$ is to be etched in a substrate. Rest part of the substrate surface is covered with a infinitely thin mask at the top to protect it from being contact with the etchant. Due to the symmetry of the problem about the center of the gap to be etched, only half of the domain is modeled in 2-D etching and one-quarter of the domain is modeled in 3-D etching as shown in Figs. 2b and 3b respectively. For ease of presentation, in the test problems 2-D and 3-D, length scales are non-dimensionalised with respect to the half gap width. The dimensionless variables used in this article are

$$X = x/a \tag{11a}$$

$$Y = y/a \tag{11b}$$

$$C = c/c_o \tag{11c}$$

$$t^* = tD/a^2 \tag{11d}$$

$$\beta = \frac{m\rho_{Sub}}{c_o M_{Sub}} \tag{11e}$$

For 1-D etching problem, the lengths of etchant and substrate domains are taken as 0.03 cm and 51 μm. The density and molecular weight of the substrate are taken to be 2.1 g/cm^3 and 60 respectively. The diffusion coefficient of etchant is 10^{-5} cm^2/sec. The stoichiometric reaction parameter is 6. In 2-D and 3-D etching problems, the dimensionless widths are taken as L_1 (l_1/a) = L_4 (l_4/a) = 6.5. The dimensionless mask thickness is $H = h/a$ = 0.005. Further decrease in mask thickness does not alter the solution. The dimensionless height of etchant above the substrate surface is taken as $L_3 = l_3/a$ = 6.5 and the substrate thickness is $L_2 = l_2/a$ = 1.0.

A grid refinement study was performed to ensure that the solutions are grid (temporal and spatial) independent. Figure 4a shows the grid independent study for 1-D etching problem with non-dimensional etching parameter, β = 1. Four spatial grid sizes are taken namely,- 12 μm, 6 μm, 3 μm, and 1.5 μm. The time step size is kept at 0.001 second and further reduction in the time step size does not alter the solution. It is seen that all four spatial grids capture the etchfront accurately. Figure 4b shows the grid independent study for 2-D problem with β = 100. The non-dimensional time step size is Δt^* = 0.01. It is seen that the grid sizes of 72 × 53 and 144 × 104 produced the same etchfront for the four given time as shown.

Figure 5 shows the comparison of etchfronts and concentration distribution in a 1-D etching problem obtained from the proposed FG method with the exact solution [7] for four β values. Figure 5a shows the temporal variation of etch depth, which varies as the square root of time. It is seen that as β increases, the etch depth increases. This is because of the increase in the initial etchant concentration with the decrease in β value, which is evident from Eq. (11e). Figure 5b shows the concentration distribution at t = 1 second.

Figure 6a shows the comparison of etchfronts in a 2-D etching problem obtained from the proposed FG method

with the existing analytical asymptotic solution [5] and the MG method [8]. The etchfronts are shown at three different non-dimensional time levels with $\beta = 100$. It is seen that the etchfronts are predicted accurately by proposed FG method. A bulging effect is seen near the mask region because of high diffusion rate of etchant near the mask region. Figure 6b shows the concentration contours for $\beta = 100$ at non-dimensional time $t^* = 30$.

Figure 7 shows the section of etchfronts for XZ- and YZ-plane cuts in a 3-D etching problem at three time levels for $\beta = 10$. The etchfronts are shown at three different sections in both plane cuts. It is seen that the etchfronts obtained from two perpendicular plane cuts are similar at same distance from the origin. This verifies the symmetry of the problem around the center of the gap. Figure 8 shows the evolution of etchfront surface for $\beta = 10$ at time level $t^* = 2.4$.

Concluding Remarks

A fixed grid method based on the total concentration of etchant has been presented to model WCE process. A brief discussion on the formulation of the problem using the proposed FG method is presented. With this proposed method the etchfront position can be found implicitly. The method has been applied to three different test problems namely,- 1-D, 2-D and 3-D diffusion-controlled etching. The results from the proposed method compared with the existing analytical and numerical approaches. The results show that etchfront can be predicted accurately using the proposed method.

REFERENCES

1. M. J. Madou, Fundamentals of microfabrication, 2nd Edition, CRC Press, New York, 2002.
2. K. S. J. Pister, M. W. Judy, S. R. Burgett and R. S. Fearing, Microfabricated hinges, Sensors and Actuators A **33**, pp. 249-256, 1992.
3. C. H. Mastrangelo, X. Zhang and W. C. Tang, Surface micromachined capacitive differential pressure sensor with lithographically-defined silicon diaphragm, The 8th International Conference on Solid-State Sensors and Actuators (Eurosensor IX), Stockholm June 25-29, pp. 612-615, 1995.
4. H. K. Kuiken, Etching: a two-dimensional mathematical approach, Proceedings of the Royal Society of London A **392**, pp. 199-225, 1984.
5. H. K. Kuiken, Etching through a slit, Proceedings of the Royal Society of London A **396,** pp. 95-117, 1984.
6. C. Vuik and C. Cuvelier, Numerical solution of an etching problem, Journal of Computational Physics **59**, pp. 247-263, 1985.
7. H. K. Kuiken, J. J. Kelly and P. H. L. Notten, Etching profiles at resist edges - I. Mathematical models for diffusion-controlled cases, Journal of the Electrochemical Society **133**, pp. 1217-1226, 1986.
8. C. B. Shin and D. J. Economou, Effect of transport and reaction on the shape evolution of cavities during wet chemical etching, Journal of the Electrochemical Society **136**, pp. 1997-2004, 1989.
9. W. J. Li, J. C. Shih, J. D. Mai, C-M. Ho, J. Liu and Y-C. Tai, Numerical simulation for the sacrificial release of MEMS square diaphragms, 1st International Conference on MSMSSA, San Jose, USA, April-1998.
10. K. Kaneko, T. Noda, M. Sakata and T. Uchiyama, Observation and numerical simulation for wet chemical etching process of semiconductor, Proceedings of 4th ASME-JSME Joint Fluids Engineering Conference, Honolulu, USA, July 6-10, 2003.
11. D. Adalsteinsson and J. A. Sethian, A level set approach to a unified model for etching, deposition and lithography I: Alogorithms and two-dimensional simulations, Journal of Computational Physics **120**, pp. 128-144, 1995.
12. D. Adalsteinsson and J. A. Sethian, A level set approach to a unified model for etching, deposition and lithography II: three-dimensional simulations, Journal of Computational Physics **122**, pp. 348-366, 1995.
13. A. La Magna, G. D'Arrigo, G. Garozzo and C. Spinella, Computational analysis of etched profile evolution for the derivation of 2D dopant density maps in silicon, Materials Science and Engineering B **102** (1-3), pp. 43-48, 2003.
14. Y. C. Lam, J. C. Chai, P. Rath, H. Zheng and V. M. Murukeshan, A fixed grid method for chemical etching, International Communications in Heat and Mass Transfer **31** (8), pp. 1123-1131, 2004.
15. P. Rath, J. C. Chai, H. Zheng, Y. C. Lam, V. M. Murukeshan and H. Zhu, A fixed-grid approach for diffusion- and reaction-controlled wet chemical etching, International Journal of Heat and Mass Transfer **48** (11), pp. 2140-2149, 2005.
16. N. Shamsundar and E. M. Sparrow, Analysis of multidimensional conduction phase change via the enthalpy method, Journal of Heat Transfer **97**, pp. 333-340, 1975.
17. A. D. Brent, V. R. Voller and K. J. Reid, Enthalpy-porosity technique for modeling convection-diffusion phase change: pplication to the melting of a pure metal, Numerical Heat Transfer **13**, pp. 297-318, 1988.
18. S. V. Patankar, Numerical Heat Transfer and Fluid Flow, 1st edition, Hemisphere, New York, 1980.

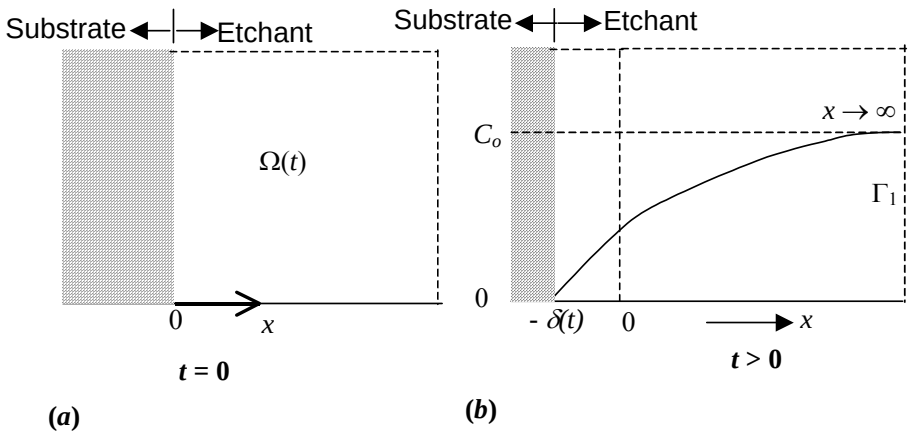

Figure 1. Schematic and computational domain of a 1-D etching problem.

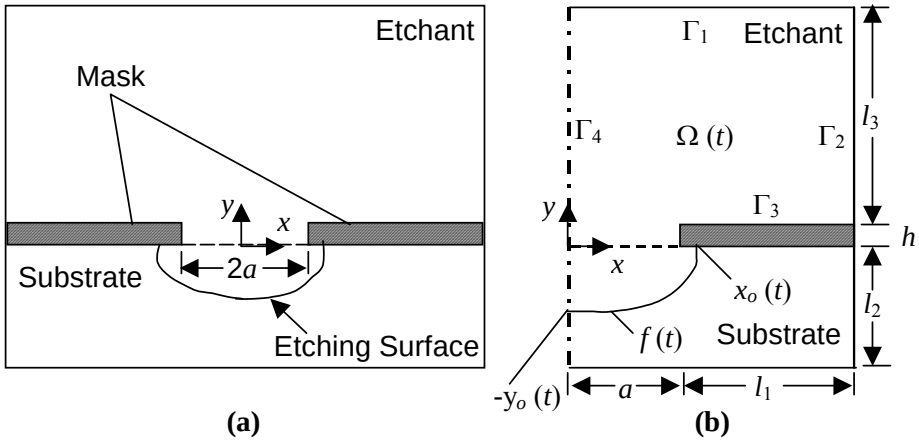

Figure 2. Schematic and computational domain of the two-dimensional (2-D) etching problem.

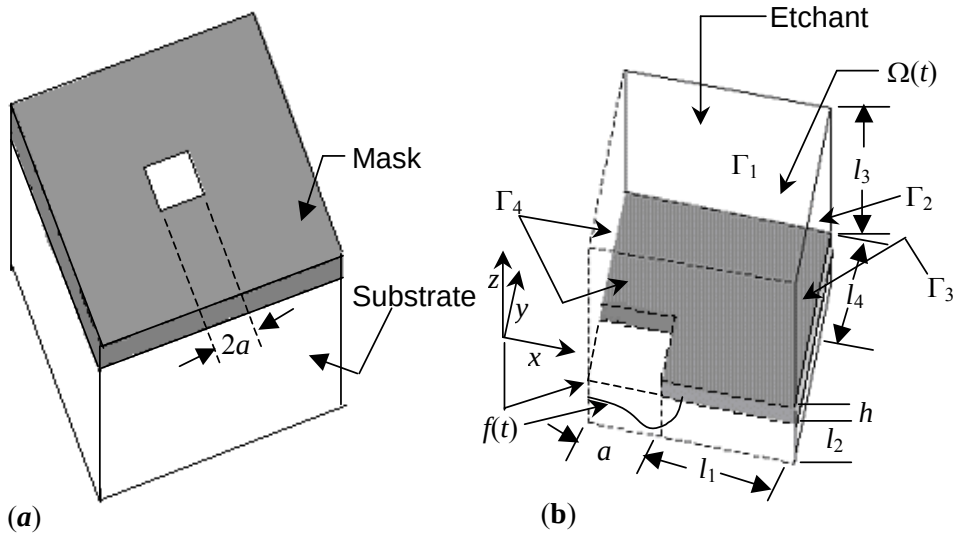

Figure 3. Schematic and computational domain of the three-dimensional (3-D) etching problem.

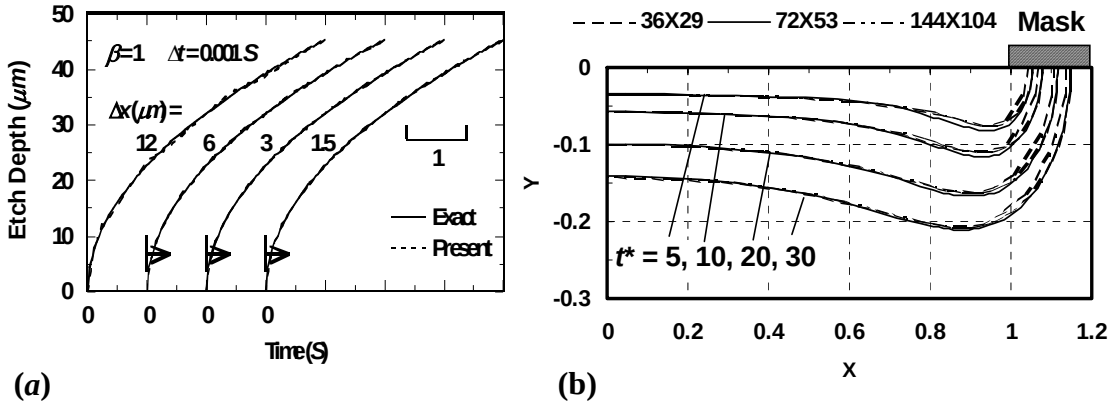

Figure 4. Grid independent test for 1-D and 2-D etching problems: (*a*) grid independent test for 1-D etching problem with β = 1, (b) grid independent test for 2-D etching problem with β = 100 and $\Delta t^* = 0.01$.

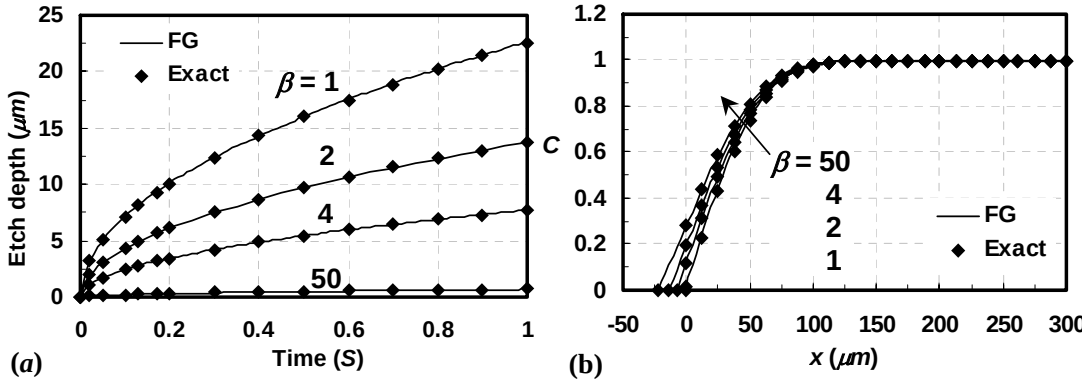

Figure 5. Comparison of etch depth and concentration distribution obtained from the proposed FG method with the exact solution: (*a*) variation of etch depth with time for four β values, (b) concentration distribution at t = 1 *S* for four β values.

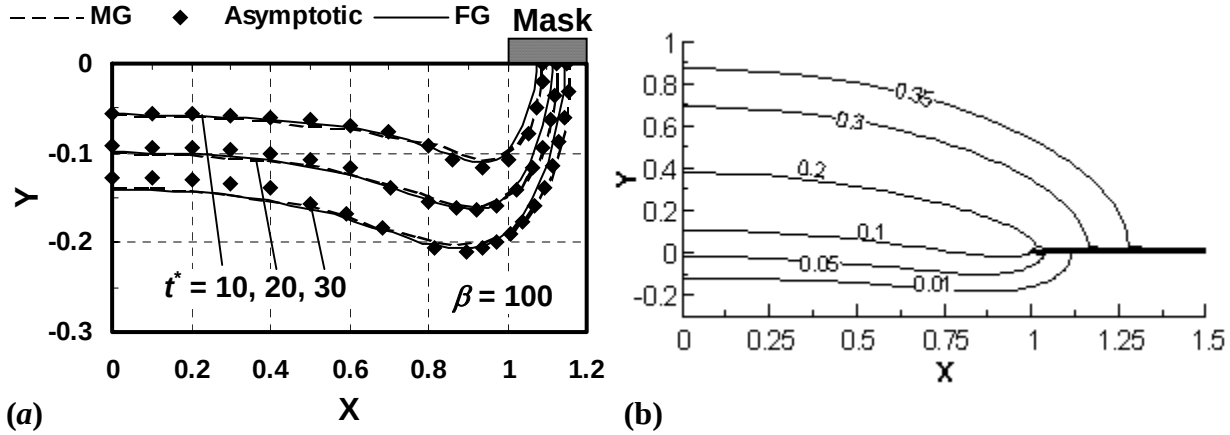

Figure 6. Etch profiles and concentration distribution in 2-D etching: (*a*) comparison of etch profiles at three different time levels obtained from the proposed FG method with analytical asymptotic solution and MG method, (b) concentration contours at $t^* = 30$ for β = 100.

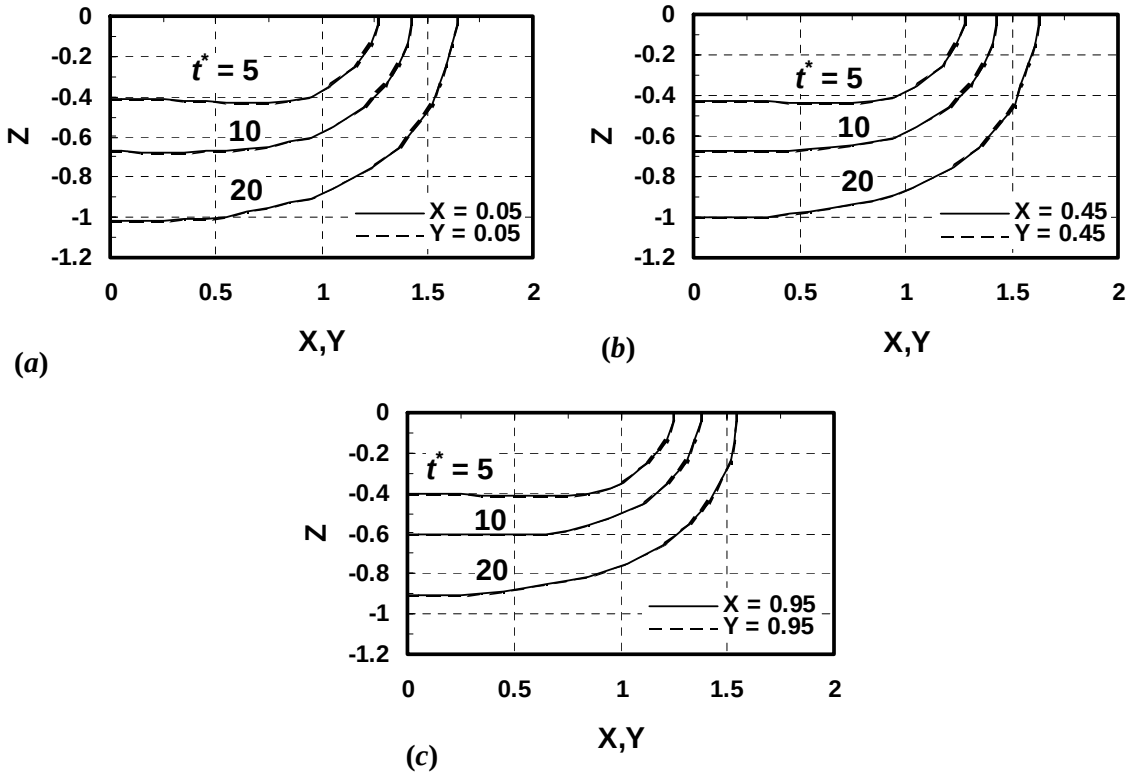

Figure 7. The etchfronts at three different locations in XZ - and YZ - plane cuts for $\beta = 10$.

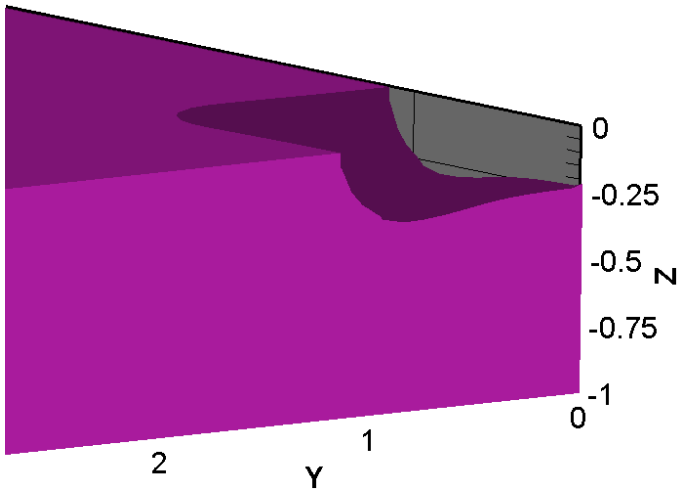

Figure 8. Evolution of etchfront surface for $\beta = 10$ at non-dimensional time $t^* = 2.4$.